A Na^+- and Cl^--activated K^+ Channel in the Thick Ascending Limb of Mouse Kidney

Marc Paulais, Sahran Lachheb, and Jacques Teulon

UPMC, CNRS UMR7134, Institut Fédératif de Recherches 58, Centre de Recherches Biomédicales des Cordeliers, Paris 75006, France

This study investigates the presence and properties of Na^+-activated K^+ (K_{Na}) channels in epithelial renal cells. Using real-time PCR on mouse microdissected nephron segments, we show that Slo2.2 mRNA, which encodes for the K_{Na} channels of excitable cells, is expressed in the medullary and cortical thick ascending limbs of Henle's loop, but not in the other parts of the nephron. Patch-clamp analysis revealed the presence of a high conductance K^+ channel in the basolateral membrane of both the medullary and cortical thick ascending limbs. This channel was highly K^+ selective ($P_K/P_{Na} \sim 20$), its conductance ranged from 140 to 180 pS with subconductance levels, and its current/voltage relationship displayed intermediate, Na^+-dependent, inward rectification. Internal Na^+ and Cl^- activated the channel with 50% effective concentrations (EC_{50}) and Hill coefficients (n_H) of 30 ± 1 mM and 3.9 ± 0.5 for internal Na^+, and 35 ± 10 mM and 1.3 ± 0.25 for internal Cl^-. Channel activity was unaltered by internal ATP (2 mM) and by internal pH, but clearly decreased when internal free Ca^{2+} concentration increased. This is the first demonstration of the presence in the epithelial cell membrane of a functional, Na^+-activated, large-conductance K^+ channel that closely resembles native K_{Na} channels of excitable cells. This Slo2.2 type, Na^+- and Cl^--activated K^+ channel is primarily located in the thick ascending limb, a major renal site of transcellular NaCl reabsorption.

The Journal of General Physiology

INTRODUCTION

Na^+-activated K^+ (K_{Na}) channels are a class of large-conductance K^+ channels of which the activity increases with the intracellular Na^+ concentration. To date, K_{Na} channel activity has been primarily reported in excitable cells, including guinea pig cardiomyocytes (Kameyama et al., 1984), and neurons from various species (for review see Dryer, 1994). It has been suggested that K_{Na} channels may either serve to control the resting membrane potential or be involved in the Na^+-dependent slow afterhyperpolarization that follows a neuronal burst of action potentials (Dryer, 1994). They are also thought to have a protective role on guinea pig cardiomyocytes under pathological conditions, such as is chemia or hypoxia (Kameyama et al., 1984). The only report of functional K_{Na} channels in a nonexcitable tissue of which we are aware is a very brief description of Na^+-activated K^+ channel activity in the plasma membrane of *Xenopus* oocytes (Egan et al., 1992a).

The recently cloned Slo2.1 (Bhattacharjee et al., 2003) and Slo2.2 (Joiner et al., 1998; Yuan et al., 2000, 2003) channels, two members of the Slo channels family, share 74% identity in the rat (Bhattacharjee et al., 2003) and display functional properties reminiscent of native K_{Na} channels in excitable cells (Joiner et al., 1998; Bhattacharjee et al., 2003; Yuan et al., 2003): channel conductance in the 140–180 pS range, the existence of several conductance substates, and the fact of being stimulated by internal Na^+. As well as being stimulated by internal Na^+, Slo2.1 and Slo2.2 channels are both coactivated by internal Cl^- (Bhattacharjee et al., 2003; Yuan et al., 2003), a yet unadressed property of native K_{Na} channels. The molecular distributions of Slo2.1 and Slo2.2 channels correlate closely with the functional observation of K_{Na} channels in excitable cells. Thus, mRNA and transcripts of both channels have been detected in the brain and, although to a lesser extent, in the heart of the mouse (Yuan et al., 2003) and rat (Bhattacharjee et al., 2003; Joiner et al., 1998). These studies also indicated a very limited distribution of channels among nonexcitable cells, as no Slo2.1 or Slo2.2 signal was detected in the spleen, lung, and liver of either rodent species. But, although Northern blot analysis also failed to demonstrate the presence of Slo2.1 mRNA in rat kidney (Bhattacharjee et al., 2003), significant levels of Slo2.2 mRNA and transcripts were unexpectedly detected in whole kidneys of the rat (Joiner et al., 1998) and mouse (Yuan et al., 2003). To date, no such large-conductance, Na^+-sensitive K^+ channels have been functionally identified in renal cells.

We therefore used real-time PCR and patch-clamp techniques on microdissected tubules of mouse nephron

Correspondence to Marc Paulais: Marc.Paulais@bhdc.jussieu.fr

Abbreviations used in this paper: CTAL, cortical thick ascending limb; MTAL, medullary thick ascending limb.

for molecular and functional characterization of renal K_{Na} channels. We report here that, in addition to excitable cells and *Xenopus* oocytes, a Na^+-activated K^+ channel is present in the membranes of epithelial renal cells. Moreover, this Slo2.2-type K^+ channel may have physiological significance, since it is primarily expressed in the thick ascending limb of Henle's loop, a major site of transcellular NaCl absorption.

MATERIALS AND METHODS

Chemicals

EDTA (dipotassium salt) and ATP (disodium salt) were from Sigma-Aldrich. EGTA was either from Research Organics Inc. or from Sigma-Aldrich.

Animal and Tissue Preparation

The experiments were conducted according to the rules of the French Ministry of Agriculture (permit no. 75–096). Male, 15–20 g, CD1 mice (Charles River Laboratories France) were fed ad libitum with a control diet (SAFE). On the day of the experiment, one mouse was killed by cervical dislocation and small pieces of renal cortex and medulla were treated with collagenase (Paulais et al., 2002).

Patch-clamp experiments were performed on the basolateral membrane of tubules microdissected as previously described (Paulais et al., 2002). For real-time PCR experiments, tubular fragments and glomeruli were microdissected at 4°C in a medium supplemented with RNase-free BSA (1 mg/ml), rinsed, and directly treated for RNA extraction (see below).

Single Channel Analysis

Current Recordings. Single-channel currents were recorded with a patch-clamp amplifier (LM-EPC 7, List Electronic; RK-400, Bio-Logic) and stored on digital audio tapes (DTR-1205, Bio-Logic). The bath reference was 0.5 M KCl in a 4% agar bridge connected to an Ag/AgCl pellet. In the cell-attached configuration, the clamp potential ($V_c = V_{bath} - V_{pipette}$) is superimposed on the cell membrane potential (V_m). In excised inside-out membrane patches $V_c = V_m$. All V_c values were corrected for liquid junction potentials, as calculated by a routine of the AxoScope software (Axon Instruments Inc.). All experiments were conducted at room temperature.

Data Analysis. Signals were typically low-pass filtered at 1 kHz by an 8-pole Bessel filter (LPBF-48DG; npi electronic GmbH) and digitized at 3 kHz by a Digidata 1200 A/D converter (Axon Instruments Inc.). The mean current (I) passing through N channels was used to calculate the normalized current (NP_o) according to the equation $NP_o = I/i$, where i is the unitary current amplitude.

For the analysis of channel kinetics, recordings were low-pass filtered at 3 kHz and digitized at 10 kHz. TAC and TACfit softwares (Bruxton Corp.) were used for semi-automatic event detection and to fit open and closed time distribution histograms, respectively. Open and closed time intervals covering a wide range (see RESULTS) fits were generated on plots of the square root of the number of observations against the logarithm of the time intervals (Colquhoun and Sigworth, 1995).

Unless otherwise stated, the maximal inward conductance (g_{in}) was determined by linear regression analysis of the i/V_c relationship between $V_c = -40$ mV and more hyperpolarizing voltages. When appropriate, the outward chord conductance (g_{out}) was defined as the slope of the i/V_c curve when measured between the reversal potential (E_{rev}) and $V_c = +60$ mV.

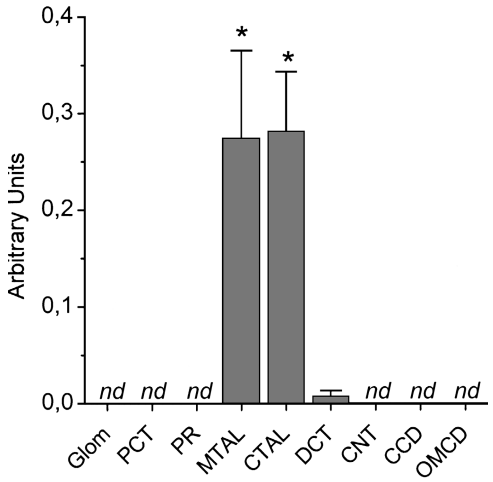

Figure 1. Intrarenal expression of Slo2.2 mRNA transcripts. Real-time PCR data are shown as mean ± SEM from 5–10 animals and are expressed in arbitrary units relative to a whole kidney RNA standard (see MATERIALS AND METHODS). *, $P < 0.05$; nd, not detectable. All samples positively responded to real-time PCR for cyclophilin (in arbitrary units): Glom 0.0147 ± 0.002 ($n = 5$), PCT 0.0424 ± 0.006 ($n = 6$), PR 0.0398 ± 0.003 ($n = 6$), MTAL 0.0192 ± 0.003 ($n = 7$), CTAL 0.0195 ± 0.002 ($n = 9$), DCT 0.0279 ± 0.003 ($n = 5$), CNT 0.0312 ± 0.0026 ($n = 10$), CCD 0.0254 ± 0.002 ($n = 10$), OMCD 0.0153 ± 0.0019 ($n = 7$).

Channel Selectivity. P_K/P_{Na} was determined in inside-out membrane patches from E_{rev} values obtained from i–V_c relationships established with opposite Na^+ and K^+ ion gradients across the membrane patch, using the Goldman, Hodgkin and Katz voltage equation (Hille, 1992):

$$E_{rev} = \frac{RT}{F} \ln \frac{[Na]_o + [(P_K/P_{Na})[K]_o]}{[Na]_i + [(P_K/P_{Na})[K]_i]},$$

where F, R, and T have their usual meanings, P_K and P_{Na} are the permeabilities to K^+ and Na^+ ions, respectively, and o and i denote the outside and inside faces of the membrane patch, respectively.

Solutions. Pipettes were typically filled with a high-K^+ solution containing (in mM) 145 KCl, 1 $MgCl_2$, 10 glucose, 10 HEPES, pH 7.4/KOH. In cell-attached patches, bath medium contained 140 NaCl, 5 KCl, 1 $CaCl_2$, 1 $MgCl_2$, 10 glucose, 10 HEPES, pH 7.4/NaOH.

The intracellular side of inside-out patches was typically bathed by a high-Na^+ medium, containing 140 NaCl, 5 KCl, 10 HEPES, 10 glucose, 2 K_2-EDTA, pH 7.4/NaOH. When appropriate (see RESULTS), various free Ca^{2+} concentrations (under constant low free Mg^{2+} concentration) were obtained by replacing EDTA with appropriate amounts of $CaCl_2$ and EGTA, as previously described (Teulon et al., 1987). In experiments where channel sensitivities to internal Na^+ and Cl^- concentrations were investigated (see RESULTS), LiCl, Li-acetate, or Na-acetate were substituted for equimolar amounts of NaCl. Na^+-induced rectification was investigated by adding appropriate amounts of NaCl to a high-K^+ solution (145 KCl, 10 HEPES, 10 glucose, 2 K_2-EDTA, pH 7.4/KOH) bathing the cytoplasmic side of inside-out patches.

Real-time PCR

mRNA was extracted from pools of 20–50 microdissected tubules or glomeruli, according to the technique previously described

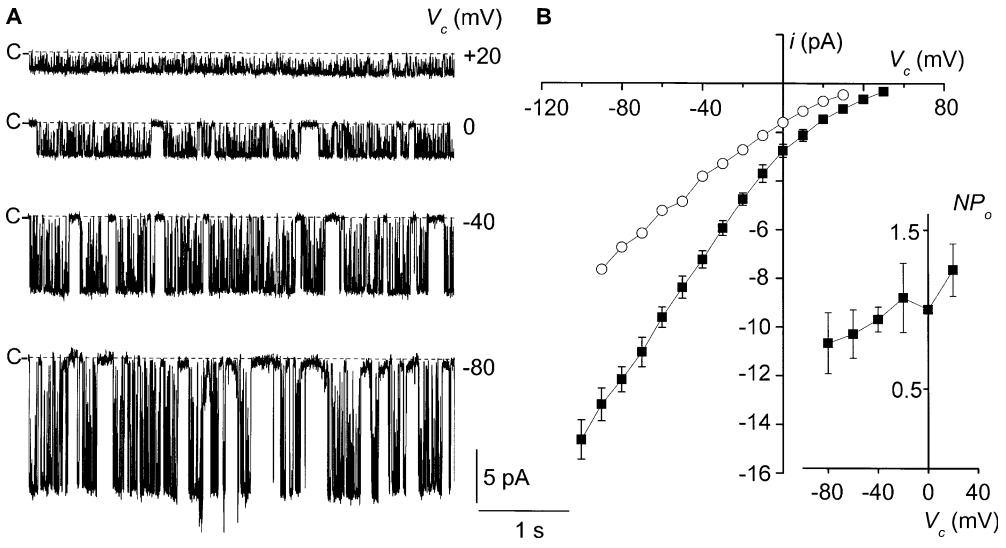

Figure 2. Properties of large-conductance K^+ channel in situ. (A) Typical recordings of large-conductance K^+ channel activity in the cell-attached membrane patch configuration. The CTAL tubule was bathed in the high-Na^+ solution, with the high-K^+ solution in the pipette. Recordings were obtained from the same membrane patch at the V_c values indicated to the right of each trace. C- is the current level corresponding to the closure of all K^+ channels. (B) Unitary current amplitude i–V_c relationships in the conditions given in A (■; n = 5–8) or in the presence of 75 mM K^+ in the pipette (○; n = 2). Inset, voltage dependence of channel activity in the conditions given in A. Channel activity is given as NP_o values normalized to that at V_c = 0 mV on the same patch. Each point is the mean of five to eight measurements and the SEM is shown as error bars when larger than symbol.

(Elalouf et al., 1993). RT was performed using the first strand cDNA synthesis kit for RT-PCR (Roche Diagnostics).

A BLAST search for the base sequence that encodes for the highly conserved region of the chloride bowl (FMFRLPFA) of human, rat, and *Caenorhabditis elegans* Slo2 channels (Yuan et al., 2003) was performed in the mouse genome. This yielded two sequences. A 3396-bp sequence was identified (GenBank/EMBL/DDBJ accession no. XM_136252), which, when translated, showed 93% homology with the amino acid sequence of rat Slo2.1 (NM_198762) (Bhattacharjee et al., 2003). A 3759-bp mouse cDNA sequence was also identified (AK048406), which, when translated, showed 99% homology with the 703–1238 amino acid sequence of rat Slo2.2 (NM_021853) (Yuan et al., 2003). The primers for the mouse Slo2.1 sequence were as follows: sense 5′-TATGATCTGCGTTGCCC-3′ (bases 747–762) and antisense 5′-CCGAACTTGCACATCC-3′ (bases 1296–1311). The primers for the mouse Slo2.2 sequence were as follows: sense 5′-AAACACAACAGCTACGAG-3′ (bases 188–205) and antisense 5′-GGGAAAAGCCGGAACA-3′ (bases 555–570). The primers for the mouse cyclophilin sequence were as follows: sense 5′-ATGGCAAATGCTGGACCAAA-3′ (bases 339–358) and antisense 5′-GCCTTCTTTCACCTTCCCAAA-3′ (bases 426–446).

Real-time PCR was performed on a LightCycler System (Roche Diagnostics) using the FastStart DNA Master SYBR Green 1 kit (Roche Diagnostics) on an 8-μl final reaction volume as previously described (Nissant et al., 2004). In brief, measurements were performed on cDNA corresponding to either 0.1 mm of tubule or 0.2 glomerulus in the presence of either 4 pmol Slo2.2 primers/8 μl or 2 pmol Slo2.1 primers/8 μl. Samples were submitted to 50 cycles of three temperatures (Slo2.2: 95°C for 10 s, 60°C for 10 s, 72°C for 20 s; Slo2.1: 95°C for 10 s, 62°C for 10 s, 72°C for 20 s). A melting curve was then established in order to check for nonspecific PCR products. After 50 cycles, no DNA was detectable in blank runs.

In each experiment, a standard curve was plotted using serial dilutions (1 to 1/500) of a cDNA stock solution obtained from mouse whole kidney RNA, dilution 1 corresponding to the cDNA produced by 10 ng RNA. For all samples, the amount of PCR product was calculated as a percentage of the RNA standard (arbitrary unit).

Data Presentation and Statistics

Results are given as means ± SEM for n experiments. P values <0.05 (paired or unpaired t test, when appropriate; SigmaPlot, SPSS) were taken to represent statistically significant differences. Nonlinear regression analyses were performed using either the SigmaPlot or the Origin (Microcal Software, Inc.) software.

RESULTS

Slo2 Channel mRNA Detection

Intrarenal expression of Slo2.1 and Slo2.2 mRNA was investigated by real-time PCR on extracts of segments microdissected from mouse nephron. No Slo2.1 mRNA was detected in any of the nephron structures tested (unpublished data). In contrast, Slo2.2 mRNA was found to be selectively expressed in the medullary and cortical thick ascending limbs (MTAL, n = 7; CTAL, n = 9) of Henle's loop (Fig. 1). No significant Slo2.2 mRNA expression was observed in glomeruli (n = 5), proximal convoluted tubules (PCT, n = 6), pars recta (PR, n = 6), distal convoluted tubules (DCT, n = 5), connecting tubules (CNT, n = 10), cortical collecting ducts (CCD, n = 10), and outer medullary collecting ducts (OMCD, n = 7). Viability of RNA samples was ascertained by real-time PCR for the house-keeping gene cyclophilin (see legend of Fig. 1).

Detection and Properties of a Large Conductance K^+ Channel in Cell-attached Membrane Patches

Using the patch-clamp technique on the basolateral membrane of collagenase-treated CTAL tubules bathed in high-NaCl solution, the activities of two types of K^+ channels were observed in situ. A previously described intermediate conductance K^+ channel (Paulais

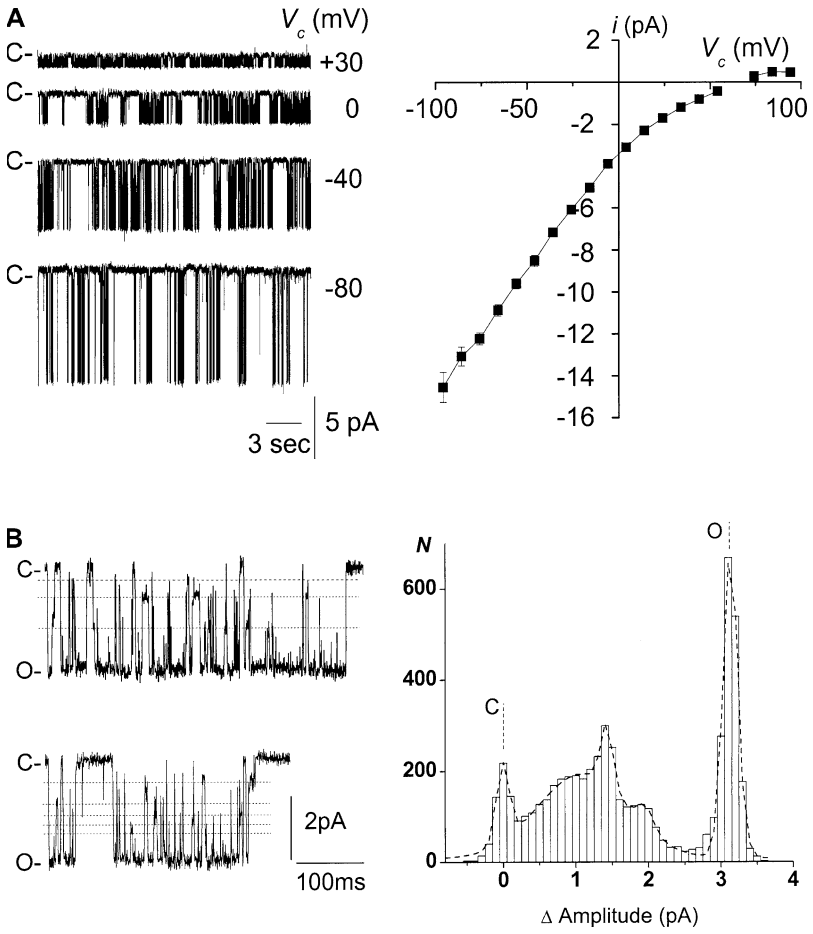

Figure 3. Large-conductance K^+ channel conductive properties in cell-excised inside-out configuration: selectivity and subconductance levels. (A, left) Typical recordings of channel activity with the high-Na^+ and low-K^+ solution in the bath, and with the high-K^+ solution in the pipette. Recordings were obtained from the same membrane patch at the V_c values given to the right of each trace. C- is the current level corresponding to the closure of all K^+ channels. (Right) Averaged i/V_c relationship under the conditions given in the left panel. Each point is the mean of 3–16 measurements and the SEM is shown as error bars when larger than symbol. (B, left) Recordings at V_c = 0 mV under the conditions given in A. Dotted lines underline subconductance levels. (Right) Corresponding amplitude histogram. C and O are the closed and complete opening levels, respectively.

et al., 2002) was observed in 27% (23 out of 85) of the patches. The activity of a larger conductance K^+ channel was also observed in ~12% (10 out of 85) of the patches. Both channel types were observed on the same patch in one case. Intermediate- and large-conductance K^+ channels were also observed on the basolateral membrane of MTAL tubules, both in 19% of the cell-attached patches (6 out of 32 patches, for each channel type). In contrast, no activity of a large conductance K^+ channel was detected in basolateral membrane of DCT (Lourdel et al., 2002). All the data presented hereafter were obtained on patches of the basolateral membrane of CTAL tubules.

Representative current tracings of large-conductance K^+ channel activity in situ and the corresponding i/V_c relationship are shown in Fig. 2. Channel conductance averaged 82 ± 6 pS at V_c = 0 mV (n = 8) and maximal inward conductance (g_{in}; see MATERIALS AND METHODS) reached 138 ± 7 pS (n = 8). No outward current was detected in these conditions and E_{rev} could be only estimated using linear regression analysis of three i/V_c relationships for inward currents. A value of 62 ± 8 mV was obtained, in good agreement with the activity of a K^+-selective channel. This was confirmed by two measurements of ionic currents with 75 mM K^+ in the patch pipette (70 mM Na^+ subsituted for K^+) (Fig. 2 B). Under these conditions, g_{in} was reduced to 83 pS and E_{rev} was shifted toward V_c ~ 42 mV. This relative shift in E_{rev} yielded a P_K/P_{Na} value >20 (for rationale see Paulais et al., 2002).

There were usually one to four active large-conductance K^+ channels in the cell-attached configuration. At V_c = 0 mV, an average of 1.8 ± 0.3 current levels were observed (n = 10), with a mean NP_o of 0.58 ± 0.11 (n = 10). Channel activity was little affected by membrane potential difference over the range studied (−80 to +20 mV), NP_o only slightly increasing in response to membrane depolarization (Fig. 2, inset).

Channel Properties in the Inside-out Configuration

Excising patches into a high-NaCl and low-KCl medium led to greater channel activity. Under theses conditions, the large conductance K^+ channel was observed on 31 out of 85 patches (36.5%). Intermediate- and large-conductance K^+ channels were observed on the same patch in seven cases (8.2%).

Representative tracings and the corresponding i/V_c curve for the large-conductance K^+ channel under these conditions are shown in Fig. 3 A. Channel conductance averaged 86 ± 2 pS at V_c = 0 mV (n = 13),

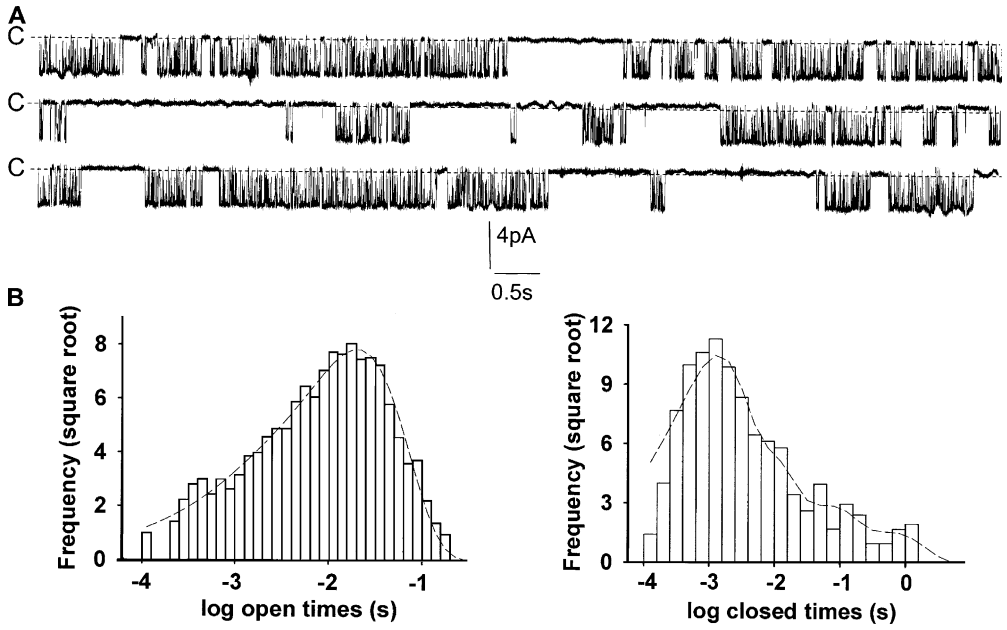

Figure 4. Channel activity and open- and closed-time distributions of cell-excised, inside-out membrane patch. (A) A continuous recording of channel activity at V_c = 0 mV. The membrane patch was bathed in the low-K^+ and high-Na^+ solution, with the high-K^+ solution in the pipette. (B) Open- and closed-time distributions of the activity shown in A. The square root of the number of events per bin was plotted against time displayed as a logarithmic function. The dashed lines are fits of the data by the sum of two (open times) or four (closed times) exponentials. The time constants and areas of the open times were 1.5 ms and 4.4%, and 19.8 ms and 95.6%, respectively. The time constants and areas of the closed times were 1.28 ms and 71.7%, 6.9 ms and 20.6%, 64.7 ms and 6%, and 601 ms and 1.8%, respectively.

and fitting the i/V_c data with the Goldman-Hodgkin-Katz current equation (Hille, 1992) yielded a g_{in} value of 154 ± 4 pS (n = 13) and an E_{rev} of 62 ± 2 mV (n = 13), confirming the K^+ selectivity of the channel with a P_K/P_{Na} ratio of 20 ± 3 (n = 13).

A feature common to K_{Na} (Mistry et al., 1996; Wang et al., 1991, Dryer 1994) and rat Slo2.1 (Bhattacharjee et al., 2003) and Slo2.2 (Yuan et al., 2003) channels is the presence of numerous subconductance levels. The examples shown in Fig. 3 B illustrate the similar behavior of the large conductance K^+ channel in the TAL. Intermediate current levels more frequently resulted from partial channel closures from the fully open state during a burst of activity, although partial openings also arose from the closed state. Within a burst, the time spent at subconductance levels accounted for 9.8 ± 1% of the total open time (n = 7).

A continuous recording on a patch containing one active channel at V_c = 0 mV is shown in Fig. 4. Typically, channel activity occurred in bursts of openings separated by closures of various duration, with no evident sign of rundown over several minutes (unpublished data). Kinetic analysis revealed that, as observed for the K_{Na} channels of excitable cells (Kameyama et al., 1984; Veldkamp et al., 1994; Mistry et al., 1997), the time distribution of the main open state was best fitted by the sum of two exponentials, longer openings being the most frequent (Fig. 4; Table I). Fitting the closed times distribution required at least four exponentials (Table I). Closures with the longest time constant were the least frequent and displayed some variability from patch to patch. Indeed, the very long and infrequent closures seen on some recordings fell outside the fitted relationship (unpublished data).

NP_o under these conditions was 0.51 ± 0.12 (n = 8) at V_c = 0 mV, with an average of 1.5 ± 0.2 channels per patch (n = 15). As observed in cell-attached membrane patches, single channel activity was moderately voltage dependent (Table I). Neither P_o nor open-time and closed-time constants and their respective proportions were significantly different when measured at V_c = 0 mV and −50 mV.

Na^+-dependent Inward Rectification

As for K_{Na} channels in guinea pig ventricular myocytes (Wang et al., 1991) and rat olfactory bulb neurons (Egan et al., 1992b), the blockade by internal Na^+ of outward currents flowing through the TAL large-conductance K^+ channel induces an inward rectification. Fig. 5 A compares single channel current amplitudes observed at V_c = +60 mV and −60 mV under symmetrical 145 mM K^+ conditions, in the presence and absence of Na^+ on the inner face of the membrane patch. In the absence of Na^+, ion currents were of similar amplitudes at both potentials. Adding 140 mM internal Na^+ had little influence on the amplitude of the inward current

TABLE I

Kinetic Parameters of Channel Activity in Inside-out Membrane Patches

Open						
V_c	n	τ_1	A_1	τ_2	A_2	P_o
mV		ms	%	ms	%	
0	4	3.05 ± 0.85	7.2 ± 2.7	16.9 ± 6.95	92.8 ± 2.68	0.33 ± 0.07
−50	3	3.4 ± 0.3	16.4 ± 4.63	8.6 ± 2.03	83.6 ± 4.63	0.15 ± 0.05

Closed									
V_c	n	τ_1	A_1	τ_2	A_2	τ_3	A_3	τ_4	A_4
mV		ms	%	ms	%	ms	%	ms	%
0	4	1.24 ± 0.11	56 ± 9.22	5.84 ± 1.33	29.1 ± 2.92	48.7 ± 10.4	12.1 ± 5.37	325 ± 86	2.93 ± 1.55
−50	3	1.51 ± 0.07	62.1 ± 1.1	14.9 ± 4.6	24.1 ± 5.1	135 ± 60.4	9.8 ± 2.4	592 ± 108	4.1 ± 2.23

Internal Na^+ concentration was 140 mM. τ_1, τ_2, τ_3, and τ_4 are time constants and A_1, A_2, A_3, and A_4 their respective proportions.

(V_c = −60 mV), but reduced the amplitude of outward current (V_c = +60 mV) by nearly 50%. Accordingly, the i/V_c relationship in the absence of Na^+ was linear over the −70 to +80 mV range, with a conductance of 177 ± 19 pS (n = 3) (Fig. 5 B). Adding 140 mM internal Na^+ reduced g_{out} to 93 ± 3 pS (n = 3; P = 0.001 vs. Na^+-free), but did not affect g_{in} (159 ± 8 pS; n = 4; P = 0.4), yielding a rectification coefficient g_{in}/g_{out} of ∼1.8.

Dependence on Internal Na^+ and Cl^-

The internal Na^+ concentration also greatly affected channel activity. This was investigated in inside-out membrane patches bathed in a low-K^+ medium, where internal Na^+ was replaced by equimolar amounts of Li^+, a cation that cannot substitute for Na^+ in activating K_{Na} channels (see Dryer, 1994). Fig. 6 shows a continuous recording of an inside-out patch initially bathed by 140 mM internal NaCl then exposed to a Na^+-free medium. With high NaCl, the activity of three large conductance K^+ channels was detected, yielding an NP_o of 0.61. When all internal Na^+ was replaced by Li^+ (the internal Cl^- being kept concentration to 145 mM), the K^+ channel currents were virtually abolished. The NP_o fell to 0.05, and there was no change in single-channel current amplitude (Fig. 6, insets). K^+ channel activity was fully and rapidly restored when internal Na^+ was reintroduced (NP_o = 0.69). The effects of internal Na^+ were concentration dependent, altering NP_o in a sigmoidal fashion (Fig. 7 A). Fitting data points using a modified Hill equation (see legend) yielded an EC_{50} of 30 ± 1 mM Na^+. A Hill coefficient n_H of 3.95 ± 0.5 was found, suggesting that the cooperative action of four Na^+ ions is required to bring about channel activation.

Rat Slo2.1 and Slo2.2 channels are both also dependent on internal Cl^-. We therefore first examined the effects of internal Na^+ concentration after reducing the internal Cl^- concentration down to 40 mM. As also illustrated in Fig. 7 A, K^+ channel activity was still dependent on the internal Na^+ concentration, but there was a clear right shift of the dose–response relationship. Under these low Cl^- conditions, EC_{50} was 74 ± 2.2 mM Na^+ and n_H was 2 ± 0.13.

Only one patch with a single active channel was seen in this experimental series. This recording, obtained under low Cl^- conditions, is shown in Fig. 7 B. It is reassuring to

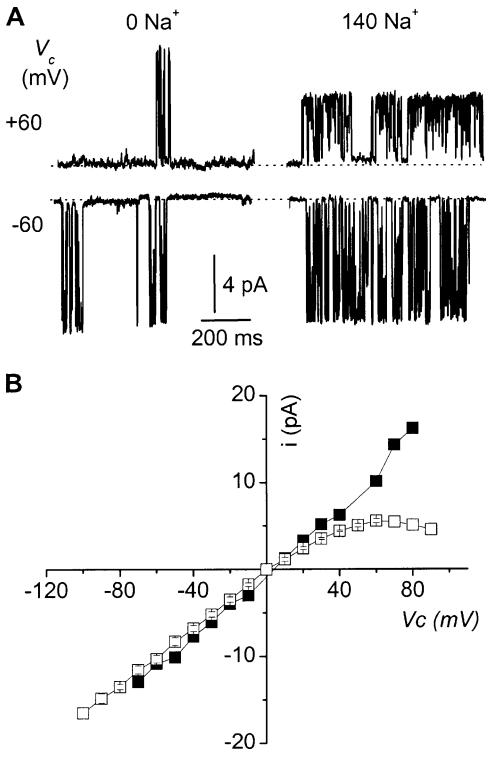

Figure 5. Na^+-induced inward rectification. (A) Single channel current tracings from inside-out membrane patches bathed in a symmetrical high-K^+ solution, at the indicated V_c values. The medium bathing the cytosolic side of the patch was either a Na^+-free medium (0 Na^+ + 5 mM K-EDTA) or a high-Na^+ medium (140 Na^+ + 5 mM K-EDTA) medium. (B) i/V_c relationships for the 0 Na (■) and 140 Na (□) conditions. Each point is the average of either 2–3 (■) or 3–4 (□) measurements. When appropriate, SEM is shown as error bars when larger than symbol.

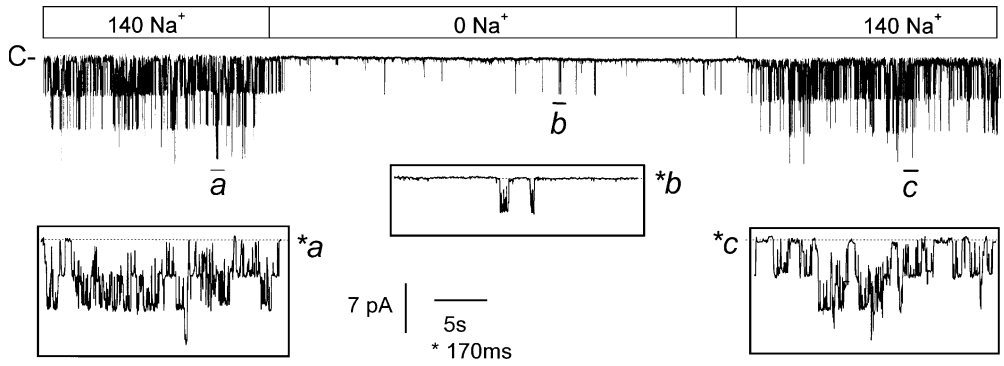

Figure 6. Na^+ dependence of channel activity. A continuous single channel recording from an inside-out membrane patch whose internal face is exposed to either a Na^+-containing medium (140 NaCl) or a Na^+-free (0 NaCl + 140 LiCl) medium. Pipette and bath K^+ concentrations were 145 and 5 mM, respectively, and V_c was set at −40 mV. C and the dotted line indicate the current level corresponding to the closure of all K^+ channels. Inset, a, b, and c, excerpts displayed at an expanded time scale (*) taken from the indicated sections of the trace.

observe that, as previously observed for K_{Na} channels in excitable cells (Kameyama et al., 1984; Mistry et al., 1997), a predominant effect of reducing internal Na^+ was an increase in the number and duration of the intervals between bursts of activity.

The concentration dependence of the effects of internal Cl^- on channel activity was then examined (Fig. 8). Under 140 mM internal Na^+ concentration, varying internal Cl^- concentration over the 0–145 mM range dose dependently affected channel activity, with EC_{50} = 35 ± 9.8 mM and n_H = 1.3 ± 0.25. These results constitute the first demonstration of a native Na^+-sensitive K^+ channel being coactivated by internal Cl^-.

Inhibition by Internal Ca^{2+} and the Lack of Effect of Internal ATP and pH

The activity of the large conductance K^+ channel was greatly dependent on the intracellular Ca^{2+} concentration. As illustrated in Fig. 9 A, we observed that channel activity was greatest in a Ca^{2+}-free medium (~1 nM free Ca^{2+}) and was reduced by increasing the free Ca^{2+} concentration. At 1 μM Ca^{2+}, NP_o was ~30% of that in Ca^{2+}-free medium (P = 0.0007; n = 4), and channel activity was further decreased by increasing free Ca^{2+} concentration to 1 mM (NP_o = 14 ± 3% of that in the Ca^{2+}-free medium; n = 6). The dose–response curve for the inhibitory effect of internal Ca^{2+} (Fig. 9 B) displayed EC_{50} ~300 nM.

Adding 2 mM Mg-ATP to the cytoplasmic side of inside-out patches for up to 1 min had no influence on channel activity (P = 0.49 ; n = 4). The effect of the internal pH (pH_i) on the activity of the channel was investigated by comparing single channel activities obtained at either pH_i 8 or pH_i 6.8 to that at pH_i 7.4. In the presence of 140 mM internal Na^+, no statistically significant influence on NP_o was observed by either decreasing or increasing pH_i (n = 3 for each condition).

DISCUSSION

Comparison with Native Na^+-activated K^+ (K_{Na}) Channels of Excitable Cells

The 150 pS Na^+-activated K^+ channel in the basolateral membrane of the mouse TAL exhibits little voltage dependence, a mild Na^+-induced rectification, several conductance substates, and is ATP and pH independent. These functional properties are similar to those commonly reported for K_{Na} channels of excitable cells and *Xenopus* oocytes (see Dryer 1994). First, the conductance of K_{Na} channels ranges from 100 to 200 pS, and the occurrence of multiple substates has been frequently reported (Wang et al., 1991; Mistry et al., 1996). Second, internal Na^+ induces an inward rectification of K_{Na} channels. The intermediate rectification coefficient (g_{in}/g_{out}) of ~2 that we observed here is close to the ratio of ~3 which can be deduced from published data on K_{Na} channels in guinea pig cardiomyocytes (Wang et al., 1991) and rat olfactory bulb neurons (Egan et al., 1992b). Third, K_{Na} channel open probability in excitable cells is usually weakly (Haimann et al., 1990; Egan et al., 1992b; Koh et al., 1994) or not (Kameyama et al., 1984; Safronov and Vogel, 1996; Mistry et al., 1997) potential dependent, and very moderately pH sensitive within the 6.5–8 pH range in the presence of an elevated internal Na^+ concentration (Veldkamp et al., 1994). Finally, K_{Na} channel activity in guinea pig cardiomyocytes (Kameyama et al., 1984) and in rat bulb olfactory neurons (Egan et al., 1992b) is not affected by internal ATP.

The activity of the 150 pS channel in the TAL increases with internal Na^+. In the presence of 145 mM internal Cl^-, the half-maximum activating Na^+ concentration (EC_{50}) and Hill coefficient (n_H) were 30 mM and 4, respectively. These values closely match the EC_{50} (30–75 mM) and n_H (2.4–4.6) values reported for K_{Na} channels of excitable membrane under similar conditions

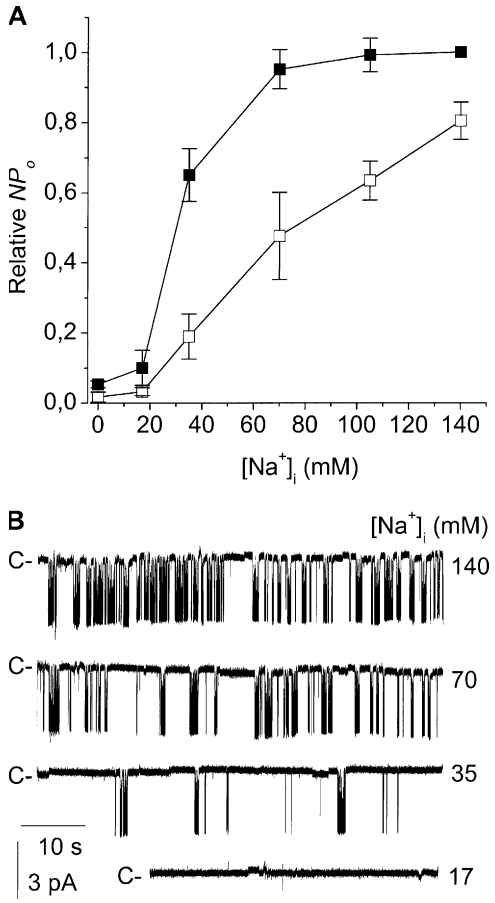

Figure 7. Internal Na^+ dependence of channel activity. (A) Dose–response relationships of the effect of internal Na^+ on the activity of the large-conductance K^+ channel. Experiments were conducted in the presence of either 145 mM internal Cl^- (■) under the conditions given in Fig. 6 or in the presence of 40 mM internal Cl^- (□). Under both conditions, the NP_o at a given internal Na^+ concentration was normalized to the NP_o obtained in the presence of 140 mM NaCl. Each point is the mean of at least three experiments, and the SEM is shown as error bars when larger than symbols. The relationships between the Na^+ concentration and NP_o were described by the equation $NP_o = 1/[1 + ([Na^+]/K)^{nH}]$, where $[Na^+]$ is the internal Na^+ concentration, K is the half-maximum activating concentration (EC_{50}), and n_H is the Hill coefficient. (B) Typical recordings of channel activity with the low-K^+ solution in the bath, and with the high-K^+ solution in the pipette. Recordings were obtained from the same membrane patch at the internal Na^+ concentrations indicated to the right of each trace. Bath Cl^- concentration was maintained at 40 mM. C- is the current level corresponding to the closure of all K^+ channels.

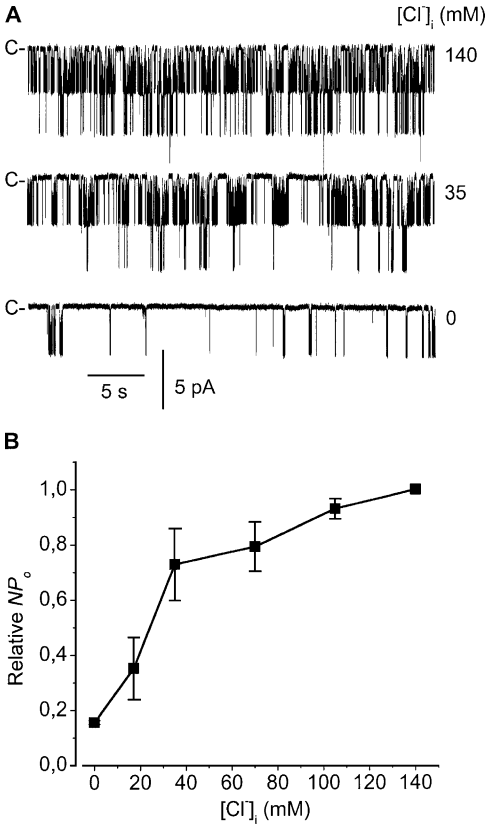

Figure 8. Internal Cl^- dependence of channel activity. (A) Typical recordings of channel activity with the low-K^+ solution in the bath, and with the high-K^+ solution in the pipette. Recordings were obtained from the same membrane patch at the internal Cl^- concentrations indicated to the right of each trace. Bath Na^+ concentration was maintained at 140 mM. C- is the current level corresponding to the closure of all K^+ channels. (B) Dose–response relationship of the effect of internal Cl^- under the conditions given in A. NP_o at a given internal Cl^- concentration was normalized to the NP_o obtained in the presence of 140 mM NaCl. Each point is the mean of three experiments, and the SEM is shown as error bars when larger than symbols.

(Dryer, 1994). These properties provide functional identification of the 150 pS K^+ channel of TAL basolateral membrane as a K_{Na} channel.

Comparison with Slo2 Channels

To date, two paralogues, *Slo2.1* and *Slo2.2*, have been shown to encode for Na^+- and Cl^--activated, large-conductance K^+ channel (Bhattacharjee et al, 2003; Joiner et al, 1998; Yuan et al, 2000, 2003). Using real-time PCR, Slo2.2 mRNA, but not that of Slo2.1, was detected in the TAL. This strongly suggests that Slo2.2 underlies the TAL K_{Na} channel.

The heterologous expression of *Slo2.1* and *Slo2.2* yields K^+ channels with very similar conductive properties (Joiner et al., 1998; Bhattacharjee et al., 2003; Yuan et al., 2000, 2003). Both genes encode for 140–180 pS K^+ channels with subconductance levels that are coactivated by internal levels of both Na^+ and Cl^-. Several functional observations confirm that Slo2.2 underlies the K_{Na} channel in the TAL. First, the Na^+-dependent activation of TAL K_{Na} channel also depends on the internal Cl^-, and reducing the internal Cl^- from 140 to 40 mM increased the EC_{50} for Na^+ from 30 to 74 mM (Fig. 7). These values are of the same order of magnitude as those reported for Slo2.2 channels under similar conditions (Yuan et al., 2003). Furthermore, Slo2.1

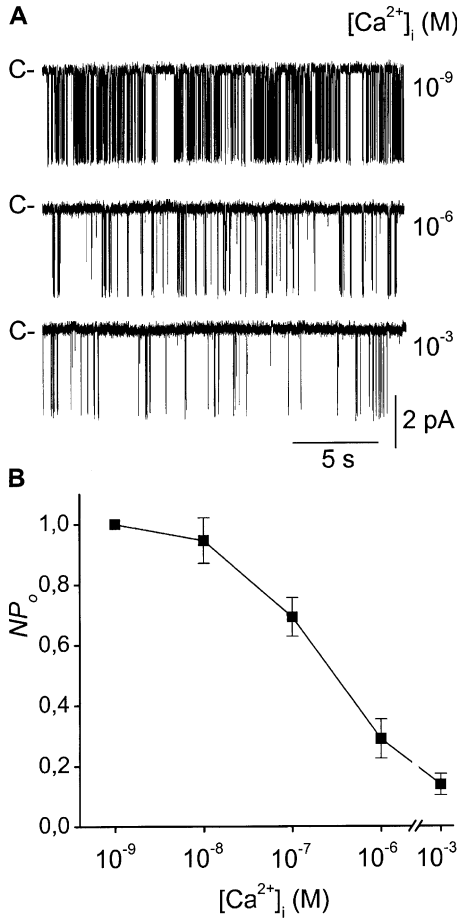

Figure 9. The activity of the K_{Na} channel in the CTAL is reduced by intracellular Ca^{2+}. (A) Single channel recordings from a cell-excised inside-out membrane patch exposed to the indicated intracellular Ca^{2+} concentration ($[Ca^{2+}]_i$). Recordings were made with a high-K^+ pipette solution and a high-Na^+ bath solution, and V_c was set at 0 mV. C indicates the current level corresponding to the closure of all K^+ channels. (B) Summary of results obtained in the conditions given in A. Each point is the mean ± SEM of 4–6 experiments. NP_o is given as the channel open probability normalized to that in 1 nM Ca^{2+} (0 Ca^{2+} + 2 EGTA).

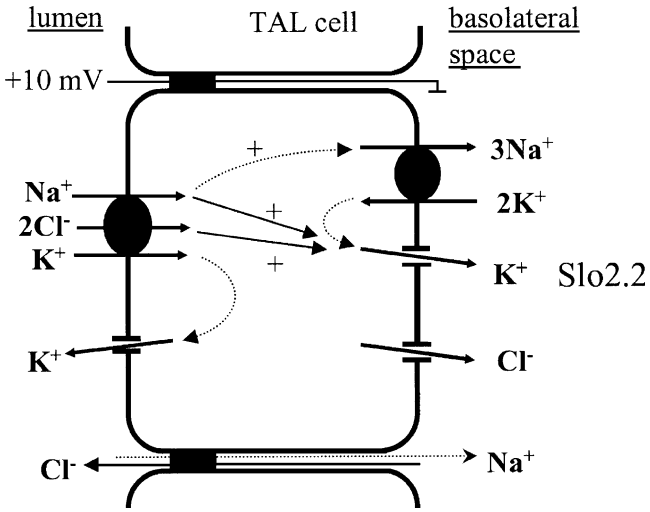

Figure 10. Simplified model of NaCl reabsorption by the TAL illustrating the possible role of the basolateral K_{Na} channel in the TAL.

displays a significant activity in a 35 mM Cl^- and Na^+-free medium (Bhattacharjee et al., 2003), whereas Slo2.2 is inactive under these conditions (Bhattacharjee et al., 2003; Yuan et al., 2003). Similar ionic conditions (0 Na^+ and 40 mM Cl^-, Fig. 7) abolished TAL K_{Na} channel activity. Also, the EC_{50} for Cl^- (35 mM, Fig. 8) we observed in the presence of an elevated internal Na^+ concentration is of the same order of magnitude as that reported for Slo2.2 channel (~20 mM Cl^-) under similar conditions (Yuan et al., 2003).

Second, Slo2.1 is inhibited by internal ATP (Bhattacharjee et al., 2003), possibly via the presence of a consensus ATP binding motif in the COOH-terminal tail of its sequence. There is no such ATP binding motif in the Slo2.2 sequences of the rat (Bhattacharjee et al., 2003) and mouse (present study). Although the possibility that ATP could inhibit rat Slo2.2 by ATP was not tested for (Bhattacharjee et al., 2003), the fact that ATP had no effect on the TAL K_{Na} channel clearly shows that this channel is not of a Slo2.1 type.

Finally, an elevation in the cytosolic free Ca^{2+} concentration inhibits rat Slo2.2 (Joiner et al., 1998). Our observation that K_{Na} channel activity in the TAL also decreased in response to an increase in the cytosolic free Ca^{2+} is also consistent with the presence of a Slo2.2 channel.

Physiological Role of a K_{Na} Channel in the TAL Basolateral Membrane

The TAL transcellularly reabsorbs 15–20% of the filtered NaCl load. Basically, NaCl enters TAL cells via an apical Na^+-K^+-2Cl^- cotransporter driven by the basolateral Na^+/K^+ ATPase and, on the basolateral side, Cl^- exits through chloride channels (Fig. 10). Basolateral K^+ channels first maintain the membrane potential difference and thus the driving force for basolateral Cl^- diffusion and, second, provide a major pathway for the efflux of K^+ ions entered into the cell by Na^+/K^+ ATPase activity. We (Paulais et al., 2002) and others (Hurst et al., 1992; Gu and Wang, 2002) have previously demonstrated the presence of an ~45 pS K^+ channel in this membrane. This channel is observed in ~30% of cell-attached patches, with an average NP_o of 1.9 and a conductance of ~10 pS under physiological conditions (Paulais et al., 2002). This makes it possible to calculate a mean conductance of ~6 pS per membrane patch. The K_{Na} channel was observed here in ~12% of the patches, with an average NP_o of 0.6. Assuming a conductance of ~45 pS under physiological conditions (Safronov and Vogel, 1996), one may calculate a conductance of ~3 pS per membrane patch. Thus, the 150 pS K^+ channel would account for ~33% of the basolateral

membrane K^+ conductance. But it should be pointed out that a significant fraction of K_{Na} channels may be inactive under resting conditions, since the channel frequency of observations increased from 12% to 35% after patch excision into a Na^+-rich medium. This may indicate that this channel is in a position to more significantly contribute to the K^+ conductance of the TAL basolateral membrane.

In situ the TAL K_{Na} channel has an NP_o of ~0.6. This observation is somewhat surprising since the Na^+ and Cl^- sensitivities we measured in cell-free patches indicate that the channel should be nearly inactive in situ. Thus, resting intracellular Na^+ and Cl^- concentrations in the TAL are ~15 mM (Rajerison et al., 1986; Lu et al., 1996) and ~35 mM (Greger et al., 1983), respectively. According to the Na^+ dependence relationship in the presence of 40 mM Cl^- in cell-free patches, channel activity is very low under these conditions. Furthermore, these later experiments were performed under Ca^{2+}-free conditions, whereas we observed that the activity of the channel was inhibited when the cytosolic free Ca^{2+} concentration was increased to a value near resting free Ca^{2+} concentration in the mouse TAL (Paulais et al., 1996). This further indicates that the TAL K_{Na} channel sensitivities to internal Na^+ and Cl^- we measured in cell-excised membrane patches are indeed underestimated, as reported for the Na^+ sensitivity of K_{Na} channel in excitable cells (Haimann et al., 1992; Rodrigo, 1993), and suggests that they may be subject to modulation. Further studies are obviously needed to identify these modulators in order to provide a more precise picture of the conditions under which it is activated, and hence its role in the reabsorption of NaCl in the TAL.

The interior of TAL cells has to cope with large fluxes of Na^+ and Cl^-. According to the TAL transport scheme, stimulating apical Na^+ and Cl^- influx is expected to produce a rapid increase in the Na^+/K^+ ATPase-mediated Na^+ efflux, and a parallel increase in basolateral K^+ conductance. Accordingly, apical and basolateral membranes must be functionally linked in order to maintain ionic reabsorption while preventing major perturbations in cellular ionic content and volume (Schultz and Lapointe, 2000). The nature of this functional linkage (or cross-talk) has been debated (Schultz and Lapointe, 2000). Numerous studies in frog skin and in amphibian and mammalian nephrons have provided evidence for the involvement of several factors, including membrane potential, cell volume, and intracellular Ca^{2+}, pH, and ATP (Schultz and Lapointe, 2000). We therefore propose that the basolateral K_{Na} channel may be involved in membrane cross-talk in the TAL by means of its sensitivity to intracellular Na^+ and Cl^- concentrations. In this case, an elevation in intracellular Na^+ and Cl^- concentrations would be expected to activate the K_{Na} channel, leading to a coupling between increased Na^+/K^+ ATPase activity and basolateral recycling of K^+.

In conclusion, the present study provides the first evidence of the presence of a K_{Na} channel in an epithelial cell membrane. So far, K_{Na} channels were thought to be present primarily in the membranes of excitable cells (Dryer, 1994). Our findings, together with the observation of K_{Na} channels in *Xenopus* oocytes (Egan et al., 1992a), may indicate that these channels have hitherto unsuspected functional roles.

We wish to thank Martine Imbert-Teboul (UMPC-CNRS, UMR7134, Paris) for help in obtaining RT-PCR measurements. The English text has been edited by Monika Gosh.

S. Lachheb holds a Ph.D. fellowship from the French Ministère de la Recherche.

Lawrence G. Palmer served as editor.

Submitted: 6 July 2005
Accepted: 13 January 2006

REFERENCES

Bhattacharjee, A., W.J. Joiner, M. Wu, Y. Yang, F.J. Sigworth, and L.K. Kaczmarek. 2003. Slick (Slo2.1), a rapidly-gating sodium-activated potassium channel inhibited by ATP. *J. Neurosci.* 23:11681–11691.

Colquhoun, D., and F.J. Sigworth. 1995. Single Channel Recordings. 2nd ed. Plenum Press, New York. 483–587.

Dryer, S.E. 1994. Na^+-activated K^+ channels: a new family of large-conductance ion channels. *Trends Neurosci.* 17:155–160.

Egan, T., D. Dagan, J. Kupper, and I.B. Levitan. 1992a. Na^+-activated K^+ channels are widely distributed in rat CNS and in *Xenopus* oocytes. *Brain Res.* 584:319–321.

Egan, T., D. Dagan, J. Kupper, and I.B. Levitan. 1992b. Properties and rundown of sodium-activated potassium channels in rat olfactory neurons. *J. Neurosci.* 12:1964–1976.

Elalouf, J.-M., J. Buhler, C. Tessiot, A. Bellanger, I. Dublineau, and C. de Rouffignac. 1993. Predominant expression of α1-adrenergic receptor in the thick ascending limb of rat kidney. Absolute mRNA quantification by reverse transcription and polymerase chain reaction. *J. Clin. Invest.* 91:264–272.

Greger, R., H. Oberleithner, E. Schlatter, A.C. Cassola, and C. Weidtke. 1983. Chloride activity in cells of isolated perfused cortical thick ascending limbs of rat kidney. *Pflugers Arch.* 399:29–34.

Gu, R.M., and W.H. Wang. 2002. Arachidonic inhibits K channels in the basolateral membrane of the thick ascending limb. *Am. J. Physiol. Renal Physiol.* 283:F407–F414.

Haimann, C., L. Bernheim, D. Bertrand, and C.R. Bader. 1990. Potassium current activated by intracellular sodium in quail trigeminal ganglion neurons. *J. Gen. Physiol.* 95:961–979.

Haimann, C., J. Magistretti, and B. Pozzi. 1992. Sodium-activated potassium current in sensory neurons: a comparison of cell-attached and cell-free single-channel activities. *Pflugers Arch.* 422:287–294.

Hille, B. 1992. Ionic Channels in Excitable Membranes. 2nd ed. Sinauer Associates, Inc., Sunderland, MA. 337–361.

Hurst, A.M., M. Duplain, and J.Y. Lapointe. 1992. Basolateral membrane potassium channels in the rabbit cortical thick ascending limb. *Am. J. Physiol.* 263:F262–F267.

Joiner, W.J., M.D. Tang, L.Y. Wang, S.I. Dworetzky, C.G. Boissard, L. Gan, V.K. Grobkoff, and L.K. Kaczmarek. 1998. Formation of intermediate-conductance calcium-activated potassium channels by interaction of Slack and Slo subunits. *Nat. Neurosci.* 1:462–469.

Kameyama, M., M. Kakei, R. Sato, T. Shibasaki, H. Matsuda, and H. Irisawa. 1984. Intracellular Na^+ activates a K^+ channel in mammalian cardiac cells. *Nature.* 309:354–356.

Koh, D.-S., P. Jonas, and W. Vogel. 1994. Na^+-activated K^+ channels localized in the nodal region of myelinated axons of *Xenopus*. *J. Physiol.* 479:183–197.

Lourdel, S., M. Paulais, F. Cluzeaud, M. Bens, M. Tanemoto, Y. Kurachi, A. Vandewalle, and J. Teulon. 2002. An inward rectifier K^+ channel at the basolateral membrane of the mouse distal convoluted tubule. Similarities with Kir4.-Kir5.1 heteromeric channel. *J. Physiol.* 538:391–404.

Lu, M., Y. Zhu, M. Balazy, K.M. Reddy, J.R. Falck, and W.H. Wang. 1996. Effect of angiotensin II on the apical K^+ channel in the thick ascending limb of the rat kidney. *J. Gen. Physiol.* 108:537–547.

Mistry, D.K., O. Tripathy, and R.A. Chapmann. 1996. The occurrence of stable subconductance levels in Na^+-activated K^+ channels in excised membrane patches from guinea-pig ventricular myocytes. *Exp. Physiol.* 81:899–907.

Mistry, D.K., O. Tripathy, and R.A. Chapmann. 1997. Kinetics properties of unitary Na^+-dependent K^+ channels in inside-out patches from isolated guinea-pig ventricular myocytes. *J. Physiol.* 500:39–50.

Nissant, A., S. Lourdel, S. Baillet, M. Paulais, P. Marvao, J. Teulon, and M. Imbert-Teboul. 2004. Heterogenous distribution of chloride channels along the distal convoluted tubule probed by single-cell RT-PCR and patch-clamp. *Am. J. Physiol. Renal Physiol.* 287: F1233–F1243.

Paulais, M., M. Baudouin-Legros, and J. Teulon. 1996. Functional evidence for Ca^{2+}/polyvalent cation sensor in the mouse thick ascending limb. *Am. J. Physiol.* 271:F1052–F1060.

Paulais, M., S. Lourdel, and J. Teulon. 2002. Properties of an inwardly rectifying K^+ channel in the basolateral membrane of mouse TAL. *Am. J. Physiol. Renal Physiol.* 282:F866–F876.

Rajerison, R.M., M. Faure, and F. Morel. 1986. Effects of external potassium concentrations on the cell sodium and potassium contents of isolated rat kidney tubules. *Pflugers Arch.* 406:291–295.

Rodrigo, G. 1993. The Na^+-dependence of Na^+-activated K^+-channels ($I_{K(Na)}$) in guinea-pig ventricular myocytes, is different in excised inside/out patches and cell attached patches. *Pflugers Arch.* 422:530–532.

Safronov, B.V., and W. Vogel. 1996. Properties and functions of Na^+-activated K^+ channels in the soma of rat motoneurones. *J. Physiol.* 497:727–734.

Schultz, S.G., and J.-Y. Lapointe. 2000. The Kidney. Physiology and physiopathology. 3rd ed., D.W. Seldin and G. Giebisch, editors. Lippincott Williams and Wilkins, Philadelphia. 569–584.

Teulon, J., M. Paulais, and M. Bouthier. 1987. A Ca^{2+}-activated cation-selective channel in the basolateral membrane of the thick ascending limb of Henle's loop of the mouse. *Biochim. Biophys. Acta.* 905:125–132.

Veldkamp, M.W., J. Vereecke, and E. Carmeliet. 1994. Effects of intracellular sodium and hydrogen ions on the sodium activated potassium channel in isolated patches from guinea pig ventricular myocytes. *Cardiovasc. Res.* 28:1036–1041.

Wang, Z., T. Kimitsuki, and A. Noma. 1991. Conductance properties of the Na^+-activated K^+ channel in guinea-pig ventricular cells. *J. Physiol.* 433:241–257.

Yuan, A., M. Dourado, A. Butler, N. Wlaton, A. Wei, and L. Salkoff. 2000. Slo-2, a K^+ channel with an unusual Cl^- dependence. *Nat. Neurosci.* 3:771–779.

Yuan, A., C.M. Santi, A. Wei, Z.W. Wang, K. Pollak, M. Nonet, L. Kaczmarek, C.M. Crowder, and L. Salkoff. 2003. The sodium-activated potassium channel is encoded by a member of the *slo* gene family. *Neuron.* 37:765–773.